DFT Studies on the Borylation of α,β-Unsaturated Carbonyl Compounds Catalyzed by Phosphine Copper(I) Boryl Complexes and Observations on the Interconversions between O- and C-Bound Enolates of Cu, B, and Si

Li Dang and Zhenyang Lin*

Department of Chemistry, The Hong Kong University of Science and Technology, Clear Water Bay, Kowloon, Hong Kong

Todd B. Marder*

Department of Chemistry, Durham University, South Road, Durham DH1 3LE, U.K.

Received July 4, 2008

The detailed mechanisms for the borylation of α,β-unsaturated carbonyl compounds, acrolein and methylacrylate, catalyzed by phosphine copper(I) boryl complexes were studied with the aid of density functional theory calculations. The results show that the catalyzed borylation occurs through C═C insertion into Cu−B to give a β-borylalkyl C-bound Cu(I) enolate intermediate. In the borylation of acrolein, the C-bound Cu(I) enolate undergoes a keto-to-enol isomerization to give an O-bound enolate intermediate followed by a σ-bond metathesis with a diboron reagent. In the borylation of methylacrylate, a keto-to-enol isomerization does not occur due to the inertness of the ester group. Alcoholysis or hydrolysis is necessary to convert the C-bound Cu(I) enolate intermediate efficiently to the borylation product and Cu(I) alkoxide that can easily undergo σ-bond metathesis with a diboron reagent. The different borylation reaction mechanisms of acrolein and methylacrylate are closely related to the relative thermodynamic and kinetic stability of the C- and O-enolate intermediates involved in the reactions of the two different classes of substrates. The insertion reactions of ethene, formaldehyde, acrolein (2-propenal, CH_2═CH−CHO), and methylacrylate (CH_2═CH−CO_2Me) into a Cu−B bond were compared. It was found that the insertion barriers correlate very well with the orbital energies of the LUMOs calculated for the four substrates, supporting the notion that the insertion mainly involves a nucleophilic attack of the Cu−B σ bond at the coordinated unsaturated substrate molecule. Although formaldehyde is more active than ethene in the insertion reaction, the reactivity of the C═C bond is greater than that of the C═O bond in α,β-unsaturated aldehyde and ester. In addition, the thermodynamics and kinetics of interconversions between O- and C-bound enolates of Cu, B, and Si have been investigated.

Introduction

Diboration reactions[1] of unsaturated compounds catalyzed by transition metal boryl complexes have attracted considerable interest over the past few decades because the reactions produce organoboron derivatives that are important intermediates in organic synthesis.[2]Among these catalyzed reactions, diboration of alkenes, alkynes, and aryl aldehydes with a diboron reagent, such as B_2cat$_2$, B_2pin$_2$, and B_2neop$_2$ (cat = catecholato = 1,2-$O_2C_6H_4$; pin = pinacolato = $OCMe_2CMe_2O$, neop = $OCH_2CMe_2CH_2O$), has been well studied both experimentally and theoretically.[3−7] A general mechanism for these reactions involves (1) insertion of a coordinated, unsaturated molecule into an M−B bond and (2) metathesis between the diboron reagent and the insertion intermediate or oxidative addition of the diboron reagent to the metal center, insertion of the substrate into one of the M−B bonds, followed by a reductive elimination involving the other boryl ligand.

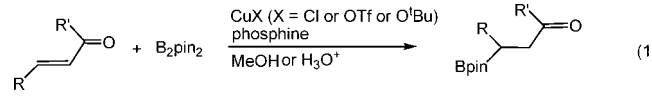

(1)

In this paper, we are interested in recent experimental studies on diboration and borylation of α,β-unsaturated carbonyl compounds[8,9]catalyzed by phosphine copper(I) complexes[8a,b,f] at room temperature (eq 1). Borylation of α,β-unsaturated carbonyl compounds with B_2pin$_2$ was also reported in the absence of phosphines, but high catalyst loadings are required.[8c,d] α,β-Usaturated carbonyl compounds have two electrophilic carbons, the carbonyl carbon and the β-carbon. Both the normal (1,2- or 3,4-addition, addition to the C═O or C═C double bond alone) and conjugate (1,4-addition, i.e., addition to the conjugated system as a whole) additions with a diboron reagent could occur. The borylation products given in eq 1 show that the β-carbon is involved, suggesting that 1,4- or 3,4-addition is responsible. It is generally believed that 1,4-addition is respon-

* Corresponding authors. E-mail:chzlin@ust.hk, todd.marder@durham.ac.uk.

(1) (a) For reviews on diboration see: Marder, T. B.; Norman, N. C. *Top. Catal.* **1999**, *5*, 63. (b) Ishiyama, T.; Miyaura, N. *Chem. Rec.* **2004**, *3*, 271. (c) Ramírez, J.; Lillo, V.; Segarra, A. M. *C. R. Chim.* **2007**, *10*, 138. (d) Burks, H. E.; Morken, J. P. *Chem. Commun.* **2007**, 4717. (e) Marder, T. B. In *Specialist Periodical Reports: Organometallic Chemistry*; Fairlamb, I. J. S., Lynam, J. M. Eds.; Royal Society of Chemistry: Cambridge, U.K., 2008, *34*, 46−57.

(2) Hall, D. G., Ed.; *Boronic Acids—Preparation, Applications in Organic Synthesis and Medicine*; Wiley-VCH: Weinheim, Germany, 2005.

10.1021/om8006294 CCC: $40.75
Publication on Web 08/14/2008

Scheme 1

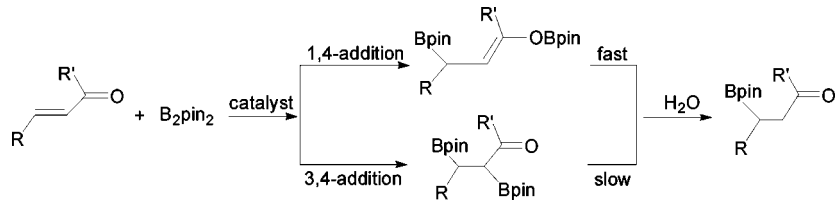

Scheme 2

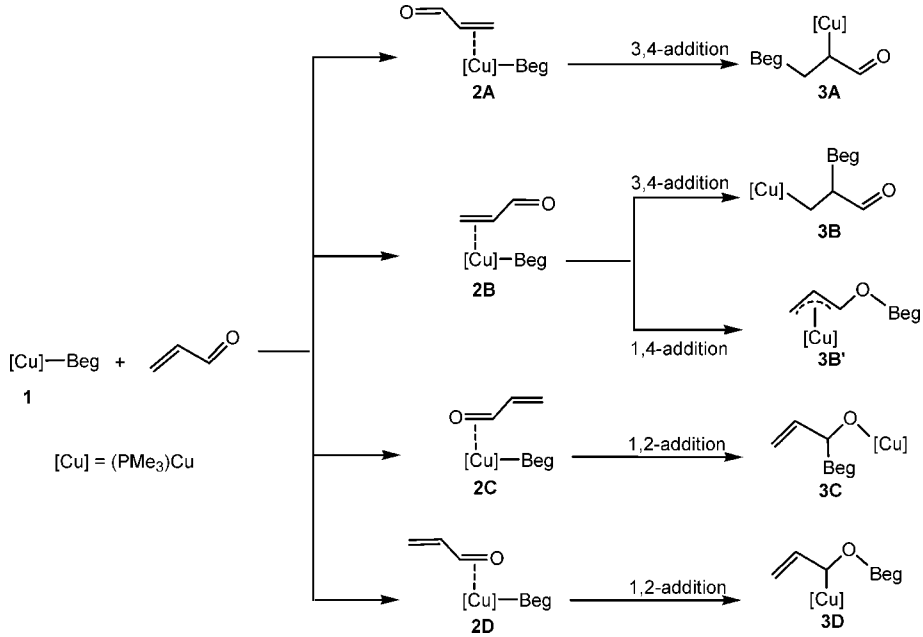

sible for the Cu(I)-catalyzed borylation reactions. However, there is no direct experimental evidence confirming such a notion. With two exceptions from our group,[9] researchers have only characterized the hydrolysis products, which are the same for 1,4- and 3,4-additions (Scheme 1), and the nature of the actual primary products is typically not known, this information being lost on hydrolysis. Indeed, we have shown[9b] that, using a diimine-Pt(0) catalyst, both 1,4- and 3,4-addition products can be formed, depending on the nature of the substrate, which hydrolyze to a common product, but at different rates (Scheme 1). As Cu is much less expensive than Pt, and the first asymmetric borylations of α,β-usaturated carbonyl compounds with a Cu catalyst have very recently been reported,[8i] we have carried out density functional theory (DFT) calculations to investigate the detailed reaction mechanism of the copper(I)-catalyzed borylation of α,β-unsaturated carbonyl compounds. Focus will be placed on the regioselectivity issue in the borylation reactions. A clear understanding of the reaction mechanism should lead to more efficient synthetic strategies.

Computational Details

Molecular geometries of the model complexes were optimized without constraints via DFT calculations using the Becke3LYP (B3LYP)[10] functional. Frequency calculations at the same level of theory have also been performed to identify all of the stationary points as minima (zero imaginary frequencies) or transition states (one imaginary frequency), and to provide free energies at 298.15 K which include entropic contributions by taking into account the vibrational, rotational, and translational motions of the species under consideration. Transition states were located using the Berny algorithm. Intrinsic reaction coordinates (IRC)[11] were calculated for the transition states to confirm that such structures indeed connect two relevant minima. The 6-311G* Pople basis set[12] was used for B in the boryl ligand and the C and O atoms in the α,β-unsaturated aldehyde substrate while the 6-311G* Wachters−Hay basis set[13] was used for Cu. For all other atoms, the 6-31G basis set was used.[14] All of the DFT calculations were performed with the Gaussian 03 package.[15] Our prior work has established the validity of using Beg (eg = $-OCH_2CH_2O-$) as a model for Bpin in catalytic reactions employing L−Cu−$B(OR)_2$ systems.[7c]

Results and Discussion

Borylation of Acrolein. It is generally believed that phosphine copper(I) boryl complexes (PR_3)Cu(boryl) are the active species in the catalytic borylation reactions shown in eq 1. The active species can be easily generated from a phosphine ligand coordination plus a metathesis reaction between the precatalyst CuX (X = Cl, OTf, or OR) and the diboron reagent. From the active species, insertion of a coordinated α,β-unsaturated carbonyl molecule into the Cu−B bond occurs. The insertion step can also be considered as addition of the Cu−B bond across a C=C or C=O double bond or the conjugated system of an α,β-unsaturated carbonyl molecule. The regioselectivity is therefore related to how the Cu−B bond is added. Transition states for five possible Cu−B additions (Scheme 2) were located from our calculations based on the model substrate H_2C=CH−CHO (acrolein) and the model phosphine copper(I) boryl complex (PMe_3)Cu(Beg) (eg = $-OCH_2CH_2O-$) (**1**). Among the five possible Cu−B additions, there are two 1,2-additions, two 3,4-additions, and one 1,4-additon. We were unable to locate the transition state related to an alternative one-step 1,4-addition in which the boryl group is added to the β-carbon and the metal fragment to the carbonyl oxygen. We explored the energetics of a few likely candidate structures for

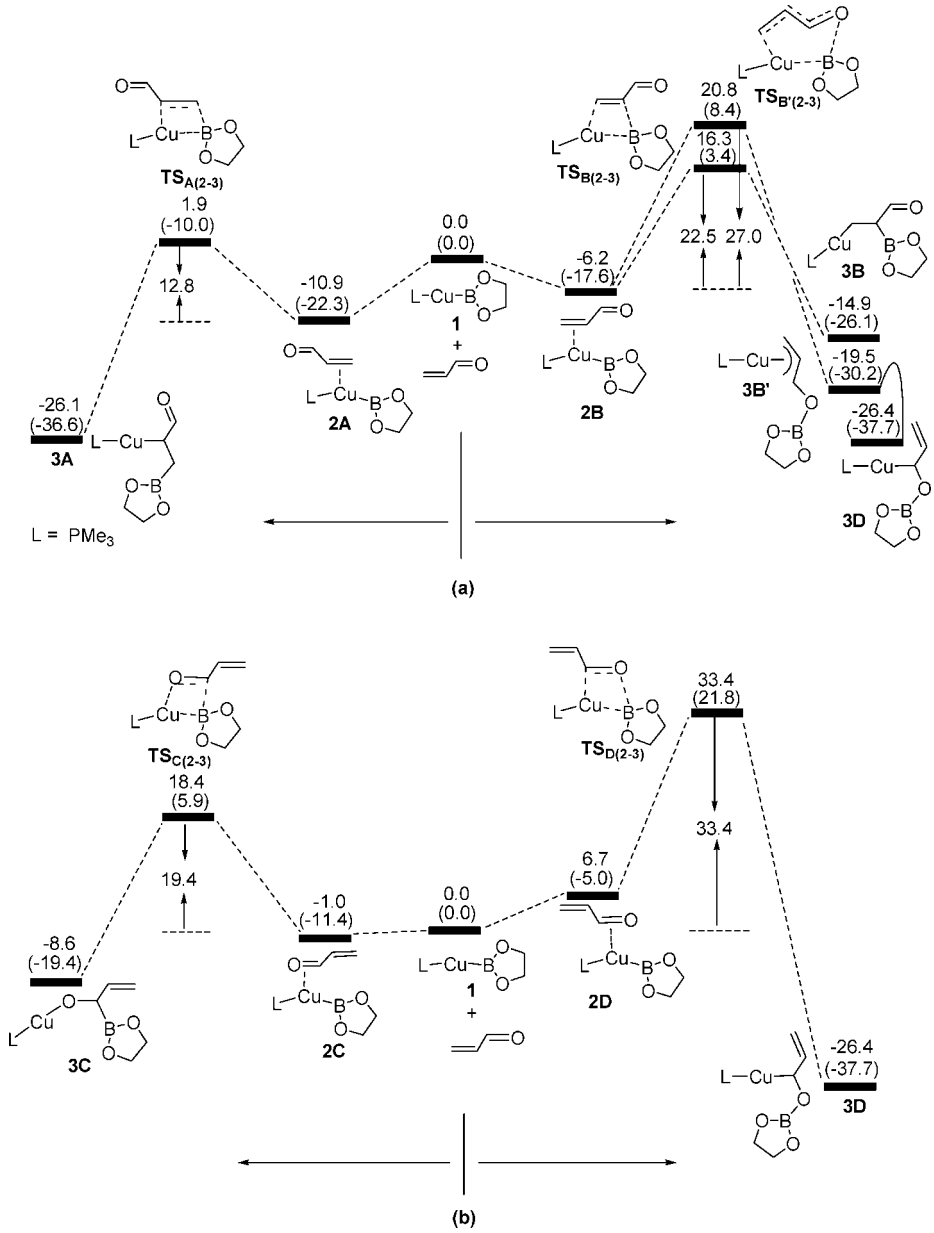

Figure 1. Energy profiles calculated for various pathways for the insertion of acrolein into the Cu−B bond of the (PMe_3)Cu(boryl) complex. The relative free energies and electronic energies (in parentheses) are given in kcal/mol.

the alternative one-step 1,4-addition transition state and found that they are highly unstable. These results suggest that even if the transition state exists, the corresponding addition is unfavorable. Figure 1 shows the energy profiles calculated for the five addition pathways in the insertion step during borylation of acrolein with B_2eg_2 catalyzed by the phosphine-ligated copper boryl model **1**. In the figure, calculated relative free energies at 298.15 K (kcal/mol) and relative electronic energies (kcal/mol, in parentheses) are presented. The relative free energies and relative electronic energies are similar in cases where the number of reactant and product molecules is equal, for example, one-to-one or two-to-two transformations, but differ significantly for one-to-two or two-to-one transformations because of the entropic contribution. The relative free energies are used to analyze the reaction mechanism in this paper. Figure 1a shows the addition pathways from the C═C coordinated intermediates **2A** and **2B** and Figure 1b shows the addition pathways from the C═O coordinated intermediates **2C** and **2D**.

The C═C coordinated intermediates **2A** and **2B** are more stable than the C═O coordinated intermediates **2C** and **2D**, indicating that the copper(I) metal center binds more strongly to the C═C double bond than to the C═O double bond in the substrate. It can be seen from Figure 1 that the 3,4-addition leading to the formation of **3A** in which the boryl group migrates to the terminal carbon of the acrolein substrate (Figure 1a) has the lowest barrier among the five addition pathways. The alternative 3,4-addition that leads to the formation of **3B** has a rather high barrier. The conjugate addition, i.e., 1,4-addition, that leads to the formation of the η^3-allyl complex **3B′**, also has quite a high barrier. **3B′** easily isomerizes to **3D** that can also be derived from a 1,2-addition shown in Figure 1b. The transition state for the isomerization is difficult to locate because the barrier is too small. Additions of the Cu−B bond in either direction across the C═O double bond of acrolein are also less favorable (Figure 1b).

To understand the above-mentioned results related to the acrolein insertion, we examined the frontier molecular orbitals, i.e., the highest occupied and lowest unoccupied molecular orbitals (HOMOs and LUMOs), of the acrolein substrate, which are shown in Figure 2. The HOMO−1 is the highest occupied

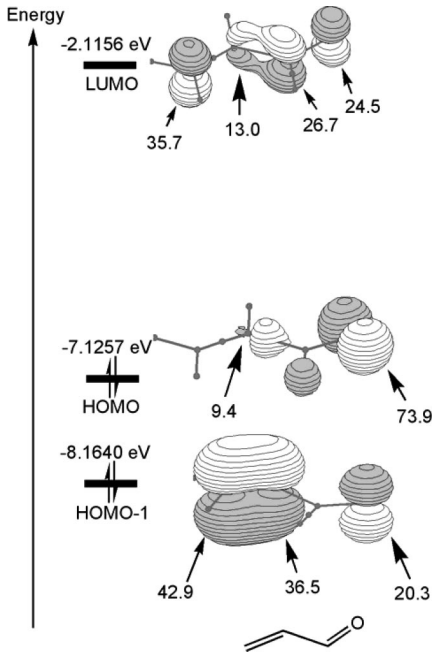

Figure 2. Frontier molecular orbitals calculated for acrolein. The orbital energies are given in eV.

π molecular orbital in the conjugated π system of the substrate, in which the C═C moiety makes the major contribution. The HOMO can be considered as the orbital accommodating the O(2p) lone pair in the carbonyl moiety of the substrate. The LUMO is the lowest π^* molecular orbital in the conjugated π system of the substrate. On the basis of the orbital features of these frontier orbitals, we can understand why the copper(I) metal center binds more strongly with the C═C double bond than with the C═O double bond in the substrate. Bonding interactions in metal−π complexes are normally described on the basis of the Dewar−Chatt−Duncanson model that emphasizes both a σ-type donation from the filled π orbital to an empty metal d orbital and a concomitant π-type backdonation from a filled metal d-orbital to the empty π^* orbital. In the highest occupied conjugated π orbital (HOMO-1) calculated for the acrolein substrate, the C═C double bond makes the major contribution. In the lowest unoccupied conjugated π^* orbital, the terminal carbon of the C═C double bond makes the highest contribution. Figure 1a shows that **2A** is more stable than **2B**. In other words, the terminal carbon of acrolein prefers to be "cis" to the Cu−B bond in the coordinated intermediate. In our previous study of the insertion of CO_2 into a Cu−B bond, we found that in the CO_2-coordinated intermediate there exists a significant backbonding interaction of the Cu−B σ bond with a CO_2 π^* orbital.[7a] The relative orientation of the acrolein ligand in **2A** allows an optimal backbonding interaction of the Cu−B bond with the lowest unoccupied acrolein π^* orbital because the terminal carbon makes the largest contribution to the π^* orbital. In the calculated structures of **2A** and **2B** shown in Figure 3, **2A** has shorter Cu−C and Cu−B bonds than **2B**. The same argument can be used to understand why **2C** is more stable than **2D**.

In our prior studies of the insertion of alkenes or aldehydes into a Cu−B(boryl) bond, we have established that the insertion mainly involves a nucleophilic attack of the Cu−B σ bond on the coordinated, unsaturated substrate molecule.[7b,d] As mentioned in the Introduction, there are two electrophilic sites in the acrolein substrate, the terminal carbon and the carbonyl carbon. On the basis of the frontier orbital analysis given above, the terminal carbon is more electrophilic than the carbonyl carbon. Therefore, as expected, the 3,4-addition, which leads to the formation of **3A**, and in which the boryl group migrates to the terminal carbon of acrolein, gives the smallest insertion barrier (Figure 1a) and the 1,2-addition with the boryl ligand attacking carbonyl carbon has the second lowest barrier (Figure 1b). The conjugate addition leads to a very stretched Cu−B bond in the transition state $\mathbf{TS_{B'(2-3)}}$ (Figure 4), resulting in a high barrier. In the transition state $\mathbf{TS_{B'(2-3)}}$, the Cu−B distance (2.10 Å) is the longest when compared with those in other transition states shown in Figure 4. The particularly high barrier

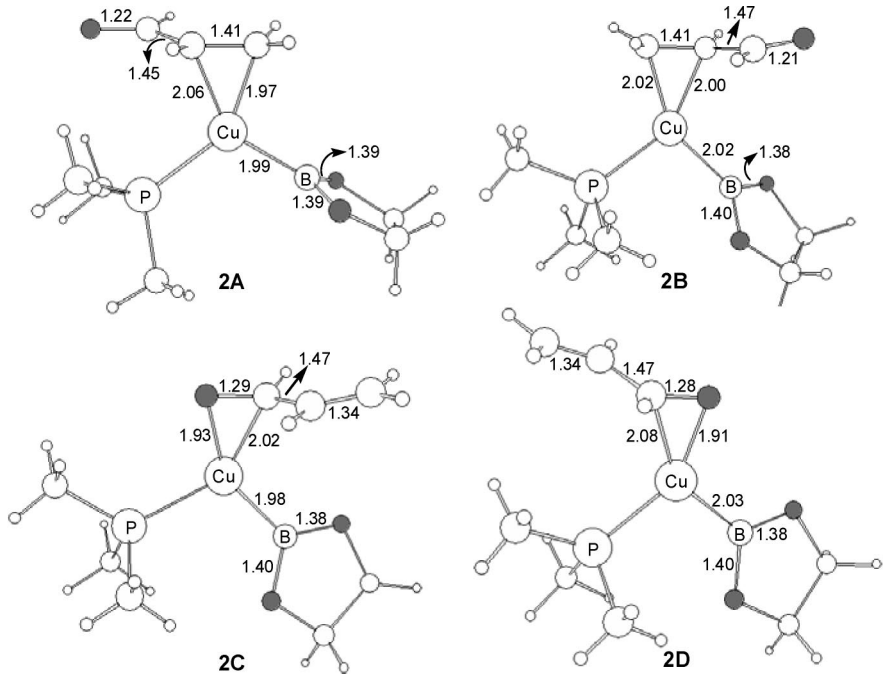

Figure 3. Optimized structures for the acrolein-coordinated intermediates with selected structural parameters (bond lengths in Å).

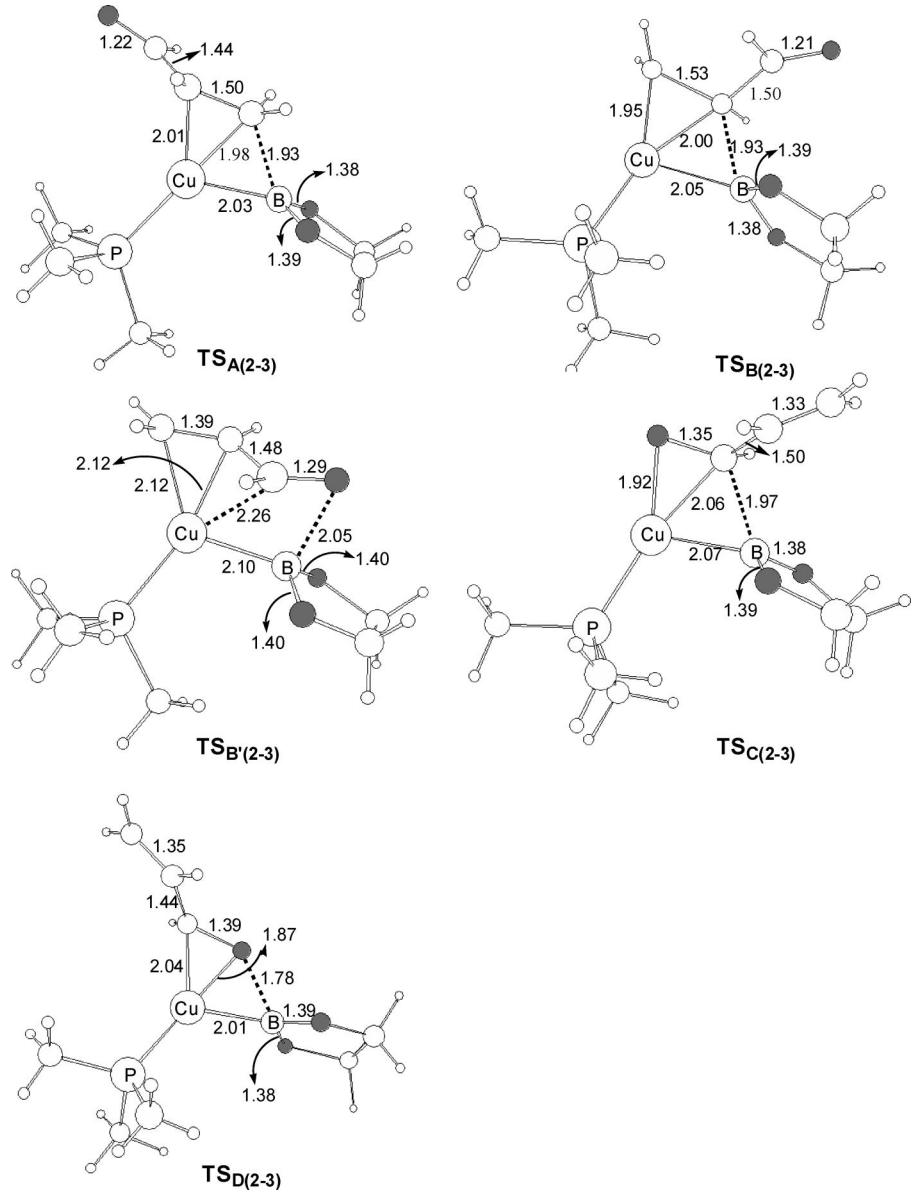

Figure 4. Optimized structures for the insertion transition states shown in Figure 1, with selected structural parameters (bond lengths in Å).

for the formation of **3D** from **2D** is related to the fact that the C═O coordinated intermediate **2D** is highly unstable (Figure 1b).

Among the five addition intermediates, **3A** and **3D** are the most stable. Figure 5 shows the structures calculated for the five addition intermediates. Careful examination of the structures shows that the Cu−C bonds in **3A** and **3D** are approximately perpendicular to the C−C═O and C−C═C planes, respectively. This structural feature suggests that **3A** and **3D** gain their stability from a conjugation interaction between the Cu−C σ bond and the C═O or C═C π bond. The conjugation interaction is evidenced by a significant shortening of the C−C single bond connecting the C═O or C═C double bond unit and the metal-bonded carbon (Figure 5). This is similar to what we saw in an α-borylalkyl Cu(I) complex in which the Cu−C σ bond also interacts with the "empty" p_z orbital on boron of the α-boryl group.[7b] Similar conjugation interaction does not exist in **3B** and **3C**, whereas **3B′** is a metastable species which easily isomerizes to **3D**, as mentioned above.

The results discussed above indicate that the 3,4-addition leading to the formation of **3A** is both kinetically and thermodynamically favorable. The 3,4-addition intermediate **3A** (the C-bound Cu-enolate) is much more stable than the reactants, and the addition is thus irreversible. Therefore, we only need to consider the addition intermediate **3A** for the steps which follow in the catalytic cycle. In addition, **3A** is a suitable synthetic target. From **3A**, a direct metathesis between **3A** and B_2eg_2 can give the 3,4-diboration product (Beg)CH_2CH-(Beg)CHO, regenerating the active species **1**. The direct metathesis requires a barrier of 24.2 kcal/mol (Figure 6). Our calculations show that **3A** can easily isomerize to the O-bound Cu-enolate form **4A** with a small barrier of 11.0 kcal/mol. **4A** can then undergo a metathesis with B_2eg_2 with a barrier of 10.2 kcal/mol to give the 1,4-diboration product (Beg)CH_2CH═CHO(Beg). Figure 6 shows that the keto-to-enol isomerization followed by a methathesis between B−B and Cu−O is much more favorable, both kinetically and thermodynamically, than a direct metathesis between B−B and Cu−C. The results are consistent with our early findings that metathesis between Cu−O and B−B is much more facile than that between Cu−C and B−B.[7d] It is interesting to note that the 1,4-diboration product (Beg)CH_2CH═CHO(Beg), i.e., the O-bound boron-enolate, is

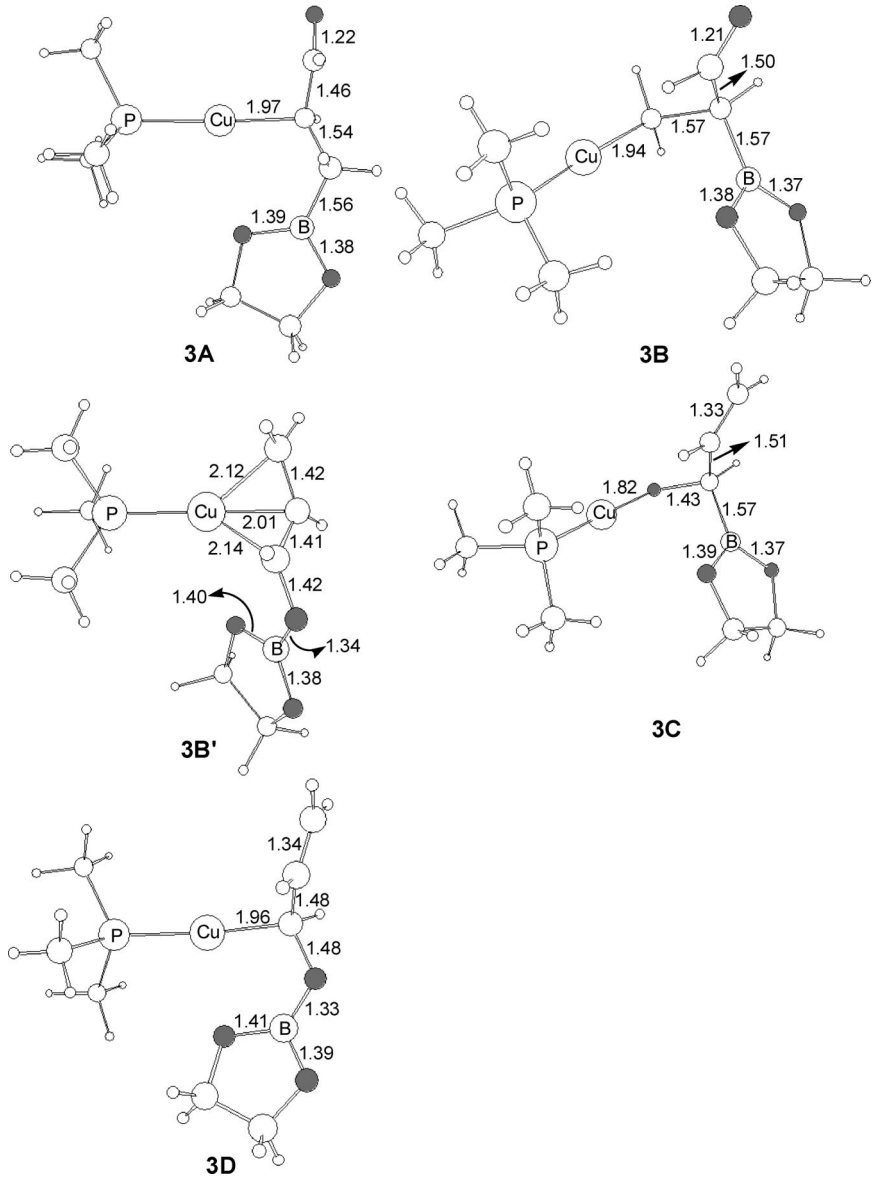

Figure 5. Optimized structures for the insertion intermediates shown in Figure 1, with selected structural parameters (bond lengths in Å).

more stable by 14.8 kcal/mol than the 3,4-diboration product (Beg)CH_2CH(Beg)CHO, i.e., the C-bound boron-enolate, likely due to the strong B−O bond in the former. Figure 7 shows the optimized structures, with selected structural parameters, for the species involved in Figure 6. Here, it is worth commenting on the two metathesis transition states $\mathbf{TS_{(3A\text{-}1)}}$ and $\mathbf{TS_{(4A\text{-}1)}}$. In $\mathbf{TS_{(3A\text{-}1)}}$, the two Cu−B bond distances are relatively short, and it can be considered as an oxidatively added transition state,[16] often found in the metathesis reactions of $L_nMR + R'-H \rightarrow L_nMR' + R-H$ if the metal center under consideration cannot easily attain a formally higher oxidation state. This is similar to what we found for the diborations of alkenes.[7c] In contrast, $\mathbf{TS_{(4A\text{-}1)}}$ has relatively long Cu−B bond distances and a relatively short B−C bond distance. According to a recent classification by Vastine and Hall of transition states for the metathesis reactions on the basis of an electron density analysis within Bader's atoms-in-molecules theory,[17,18] we can easily assign $\mathbf{TS_{(3A\text{-}1)}}$ and $\mathbf{TS_{(4A\text{-}1)}}$ to classes **E** (OATS/OHM, oxidatively added transition state[16]/oxidative migration[19]) and **C** (σ-CAM, σ-complex assisted metathesis[20]), respectively.

Based on our calculations, the catalytic cycle shown in Scheme 3 is formulated. Borylation of acrolein catalyzed by copper(I) boryl complexes involves acrolein coordination and insertion into the Cu−B bond, a keto-to-enol isomerization, and a metathesis step to regenerate the active catalyst.

Role of Methanol or Water in the Catalytic Cycle. Experimentally, it was found that addition of alcohols significantly promotes the copper-catalyzed β-borylation of α,β-unsaturated carbonyl compounds.[8f] In addition, as mentioned in the Introduction, hydrolysis was normally carried out in order to characterize the borylation products in the reactions.[8] Therefore, it is necessary to study the effect of methanol or water on the catalysis. We chose to study how a methanol molecule affects the steps involved in the catalytic cycle shown in Scheme 3.

We first examined the stability of the active species (PMe_3)Cu(Beg) (**1**) in the presence of MeOH. Metathesis of **1** with MeOH could give a copper alkoxide (**5A**) and HBeg or a copper hydride (**6A**) and MeOBeg. The energy profiles are shown in Figure 8a, giving barriers of 24.0 and 31.7 kcal/mol,

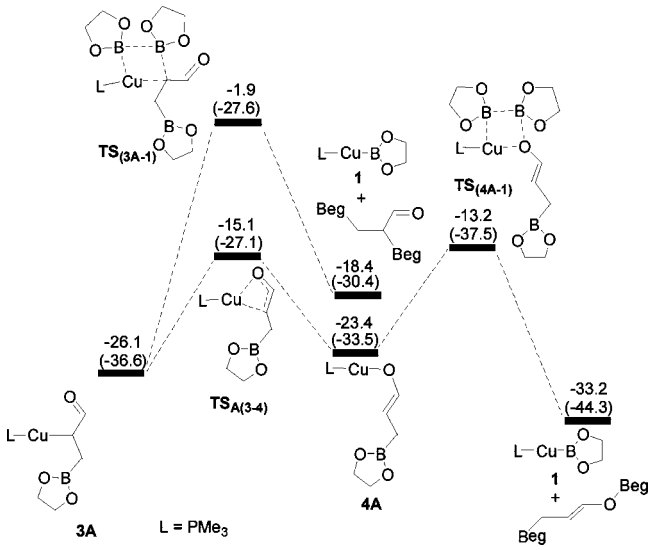

Figure 6. Energy profiles calculated for the **3A** →**4A** keto-to-enol isomerization process and for the metathesis pathways from **3A** and **4A**. The relative free energies and electronic energies (in parentheses) are given in kcal/mol.

respectively. The barriers calculated are significantly higher than the barrier of 12.8 kcal/mol calculated for the most favorable addition step (**2A** → **3A**, Figure 1). Since the addition step is irreversible as discussed above, we can conclude that the presence of MeOH will not affect the reactivity of the active species **1**.

Hydrolysis or alcoholysis can also occur with the intermediates **3A** and/or **4A**. Figure 8b shows the energy profile calculated for the reaction of **3A** with methanol. A six-membered-ring hydrogen-bonded intermediate **7A** is formed initially. Then, a proton transfer occurs to give a new hydrogen-bonded species **9A**. We failed to locate the transition state from **7A** to **9A**. A relaxed potential energy surface scan from **9A**, along the O−H reaction coordinate, suggests that the barrier for the reverse process is negligibly small. An enol-to-keto tautomerization in **9A** can occur easily to give **5A** and the β-borylated product. From **5A**, a metathesis with B_2eg_2 easily regenerates the active species **1**. Our earlier study showed that the barrier for the metathesis reaction between Cu−OMe and B_2eg_2 is less than 5 kcal/mol.[7c] Figure 8c shows the energy profiles for the reaction of **4A** with methanol. Two possible pathways were studied, one involving a 2 + 2 addition and the other via a six-membered-ring transition state. The two pathways have similar reaction barriers and easily give **5A** followed by a metathesis with B_2eg_2 to regenerate the active species **1**.

The results described above indicate that alcoholysis or hydrolysis can occur with **3A** and/or **4A** as the barriers associated are smaller than that of the addition step (**2A** → **3A**) and are comparable with or slightly smaller than the barriers

Scheme 3

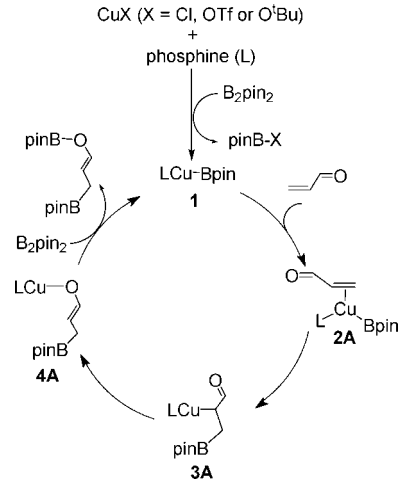

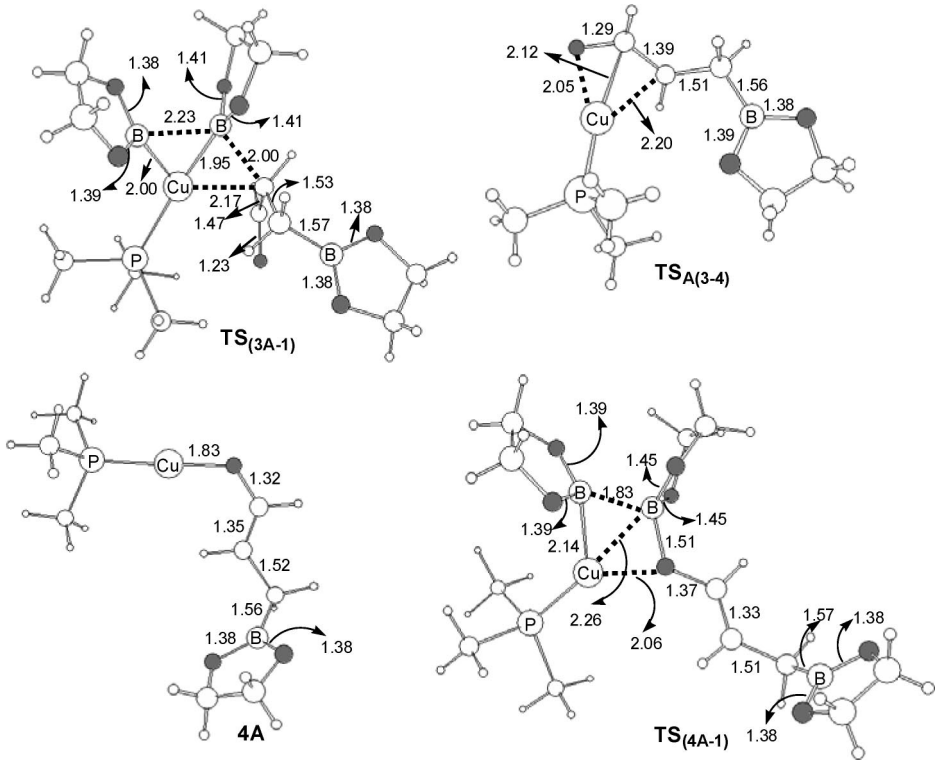

Figure 7. Optimized structures, with selected structural parameters (bond lengths in Å), for the species shown in Figure 6.

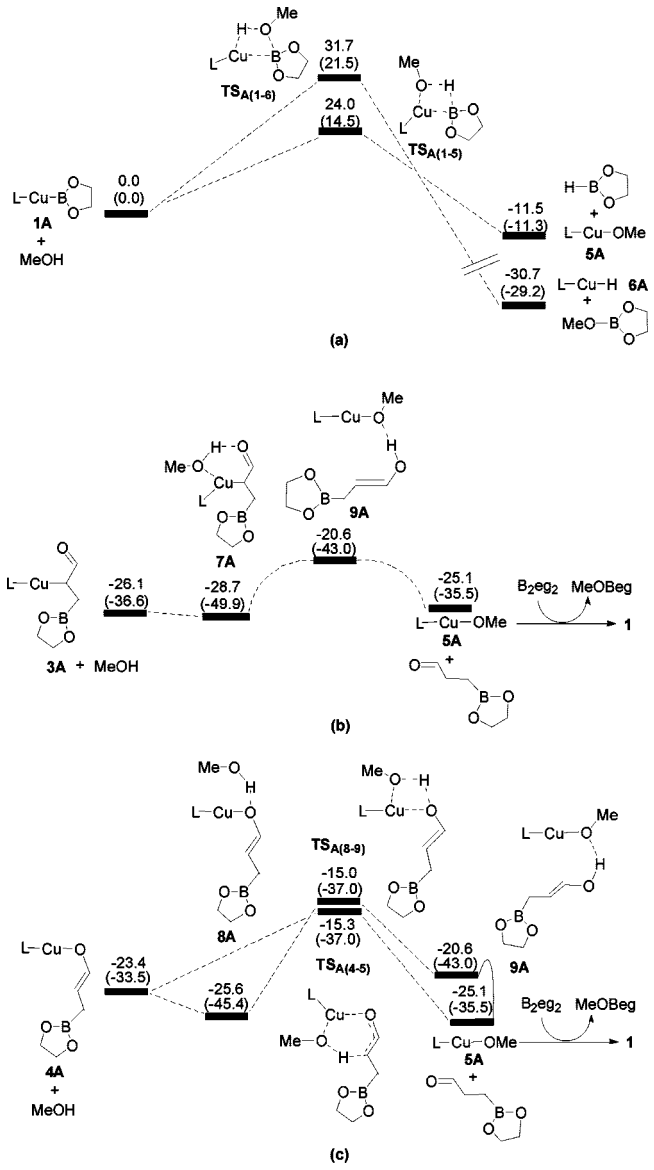

Figure 8. Energy profiles calculated for the reactions of **1**, **3A** and **4A** with methanol. The relative free energies and electronic energies (in parentheses) are given in kcal/mol.

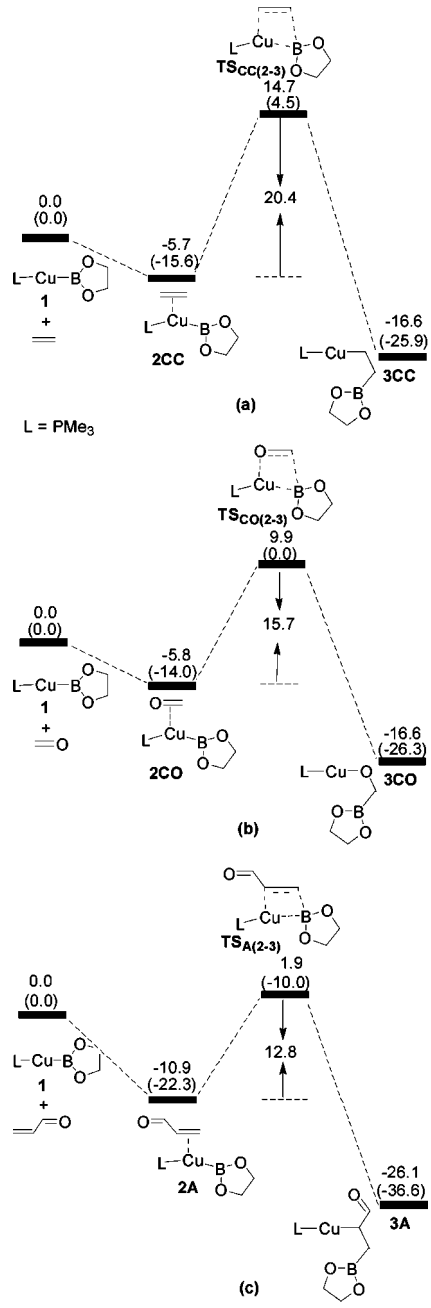

Figure 9. Comparison of the energy profiles for the insertion reactions of ethene, formaldehyde, and acrolein into the Cu−B bond of the (PMe$_3$)Cu(boryl) complex. The relative free energies and electronic energies (in parentheses) are given in kcal/mol.

Scheme 4

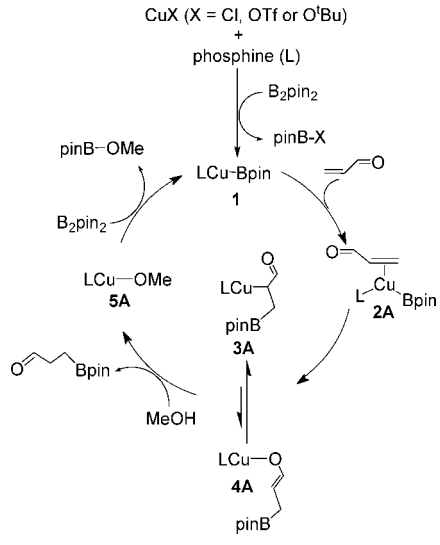

from **3A** to **4A** and **4A** to **1** (Figure 6). Scheme 4 gives a new catalytic cycle showing the role played by methanol in the mechanism of the borylation of acrolein.

Comparison of the Insertion Reactions of $H_2C{=}CH_2$, H_2CO, and $H_2C{=}CH{-}CHO$. α,β-Unsaturated aldehydes contain both C=C and C=O moieties. Therefore, it is interesting to compare the insertion reaction of acrolein with those of ethene and formaldehyde, which we studied previously.[7b,d] The energy profiles calculated for the insertion reactions of ethene, formaldehyde, and acrolein into the Cu−B bond of the model phosphine copper(I) boryl complex (PMe$_3$)Cu(Beg) **1** are shown in Figure 9. The three substrates coordinate easily with the copper center to form the three intermediates **2CC**, **2CO**, and **2A** (Figure 9). Among the three substrates, acrolein forms the most stable intermediate and has the smallest insertion barrier.

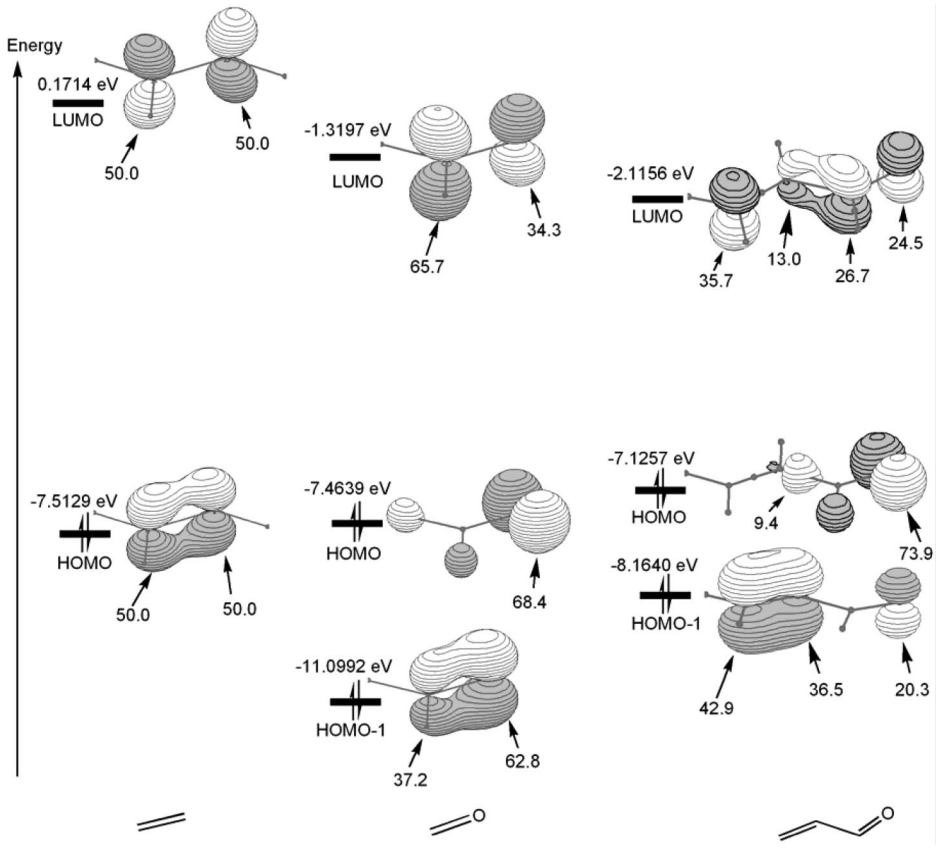

Figure 10. Frontier molecular orbitals calculated for ethene, formaldehyde, and acrolein. The orbital energies are given in eV.

With respect to their reactants, the ethene- and formaldehyde-coordinated intermediates **2CC** and **2CO** have similar stability. Ethene has the highest insertion barrier.

To understand the results summarized above, we compared the frontier molecular orbitals calculated for the three substrates (Figure 10). The three insertion barriers correlate very well with the orbital energies of the LUMOs calculated for the three substrates, further supporting the notion that the insertion mainly involves a nucleophilic attack of the Cu−B σ bond on the coordinated unsaturated substrate molecule.

Acrolein forms the most stable intermediate **2A**, due to (1) its low lying LUMO which allows stronger metal-to-ligand backbonding, and (2) its reasonably high lying occupied conjugated π orbital (HOMO-1) used for the ligand-to-metal donation interaction as discussed earlier. Ethene has the highest energy LUMO, and the backbonding interaction in **2CC** is expected to be the weakest among the three substrate-coordinated intermediates. However, it has the highest HOMO among the three substrate, leading to stronger ligand-to-metal donation interaction in **2CC**. As a result, the ethene- and formaldehyde-coordinated intermediates **2CC** and **2CO** have similar stability with respect to their reactants.

For the insertion reactions of ethene and formaldehyde, we see that formaldehyde is more active than ethene. However, for acrolein, which contains both C=C and C=O bonds, the insertion reactivity of the C=C bond is greater than that of the C=O bond.

Borylation of Methylacrylate. Up to this point, we have limited our discussion to acrolein. We expect that the results obtained should be applicable to α,β-unsaturated aldehydes or ketones. However, when α,β-unsaturated esters are considered, certain mechanistic aspects can be very different. The relatively inert ester groups are expected to make the corresponding keto-to-enol isomerization (see **3A** → **4A** in Figure 6) less likely.

Figure 11a shows the energy profiles related to the reaction of B_2eg_2 with methylacrylate, a model α,β-unsaturated ester substrate, catalyzed by **1**. Similar to what we have seen for the borylation of acrolein, **1** first coordinates with the ester substrate through the C=C π bond to form **2Aester**, from which insertion into the Cu−B bond then occurs to give the insertion intermediate **3Aester**. The binding energy of methylacrylate to **1** (−10.3 kcal/mol) and the insertion barrier (13.6 kcal/mol) are comparable with those calculated for acrolein (see **1** → **2A** → **3A** in Figure 1). As expected, in contrast to what we found for acrolein, the enol form **4Aester** here is highly unstable with respect to the keto form **3Aester** due to the relatively inert ester group. The metathesis between **4Aester** and B_2eg_2 also has a higher barrier (17.2 kcal/mol) than that between **4A** and B_2eg_2 (10.2 kcal/mol). The instability of the enol form **4Aester** and the high metathesis barrier lead to a very high overall barrier (31.9 kcal/mol) for the process from the insertion intermediate **3Aester** to the point where the active species **1** is regenerated. A direct metathesis between **3Aester** and B_2eg_2 to give a 3,4-addition product was also calculated to have a high barrier (26.4 kcal/mol), higher than that calculated for the metathesis between **3A** and B_2eg_2 (24.2 kcal/mol, Figure 6).

On the basis of the results shown in Figure 11a, we do not expect that α,β-unsaturated esters are good substrates for borylation calatyzed by phosphine Cu(I) boryl complexes in view of the high barriers calculated. Experimentally, it was found that addition of methanol greatly enhances the efficiency of the β-borylation of α,β-unsaturated esters.[8f] Figure 11b shows the energy profiles related to alcoholysis of the insertion intermediate **3Aester**. A direct 2 + 2 alcoholysis via the transition state $\mathbf{TS_{Aester(3-5)}}$ has a high barrier and is unlikely.

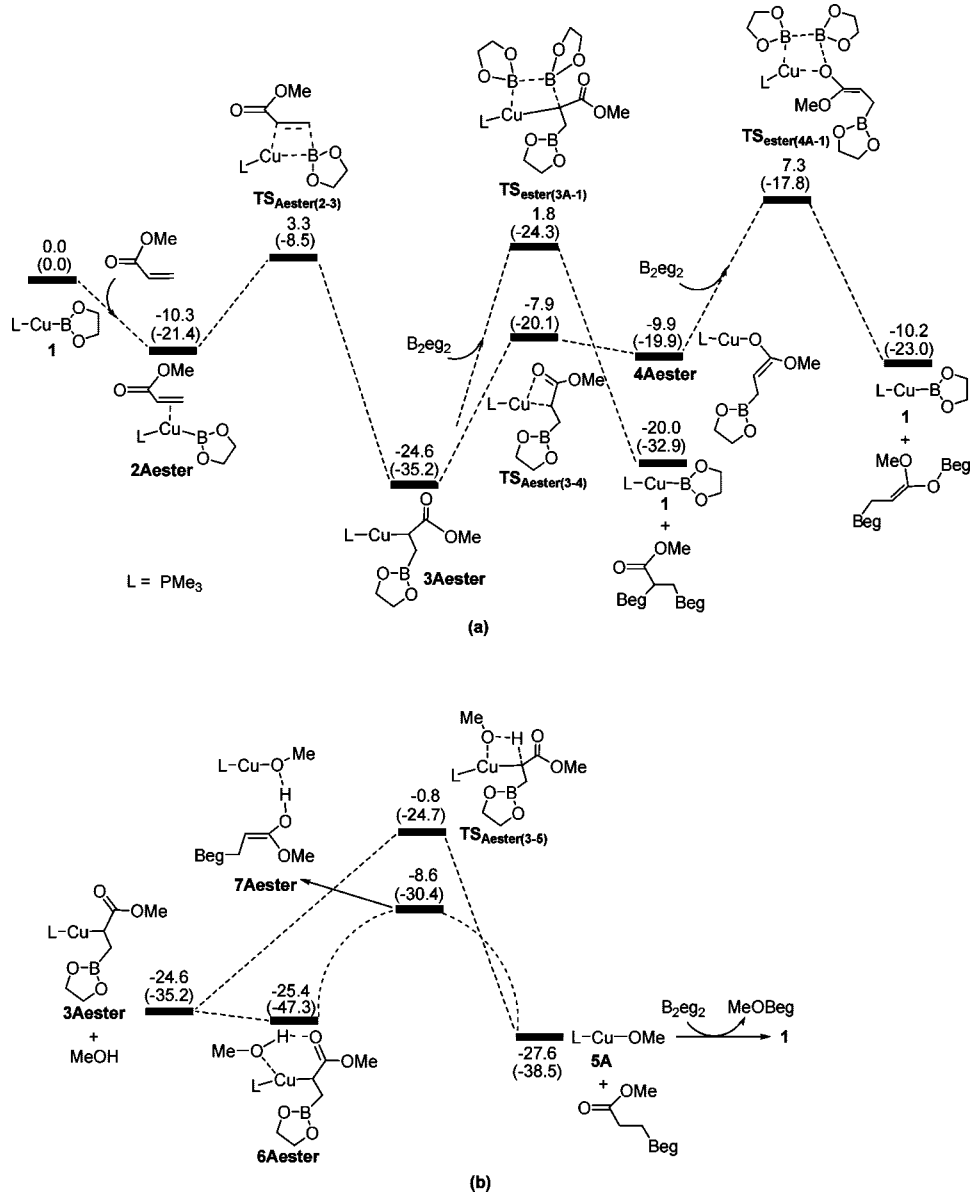

Figure 11. (a) Energy profiles related to the reaction of B_2eg_2 with methylacrylate, a model of α,β-unsaturated ester substrate, catalyzed by **1**. (b) Energy profiles calculated for alcoholysis of **3Aester** with methanol. The relative free energies and electronic energies (in parentheses) are given in kcal/mol.

Scheme 5

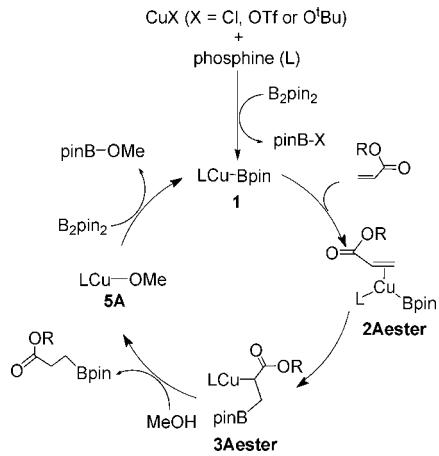

The pathway via a six-membered-ring hydrogen-bonded intermediate **6Aester** is favorable for the alcoholysis process. From **6Aester**, a proton transfer occurs to give a new hydrogen-bonded species **7Aester**. Similar to what we have seen in the alcoholysis of **3A**, we also failed to locate the transition state from **6Aester** to **7Aester**. Again, a relaxed potential energy surface scan from **7Aester** along the O−H reaction coordinate suggests that the barrier for the reverse process is negligibly small. An enol-to-keto tautomerization in **7Aester** can easily occur to give **5A** and the β-borylated product. From **5A**, a metathesis with B_2eg_2 easily regenerates the active species **1**. The results suggest that the alcoholysis here is the rate-determining step. Scheme 5 summarizes the catalytic cycle for the catalyzed borylation of α,β-unsaturated esters.

Thermodynamic and Kinetic Stability of C- and O-enolates. The detailed calculations allow us to examine the subtle difference in mechanistic aspects between the borylation reactions of α,β-unsaturated aldehydes/ketones and esters. The mechanistic difference is mainly due to the different relative stability of the keto and enol intermediates relevant in the reactions of the two different classes of substrates. For acrolein,

Scheme 6

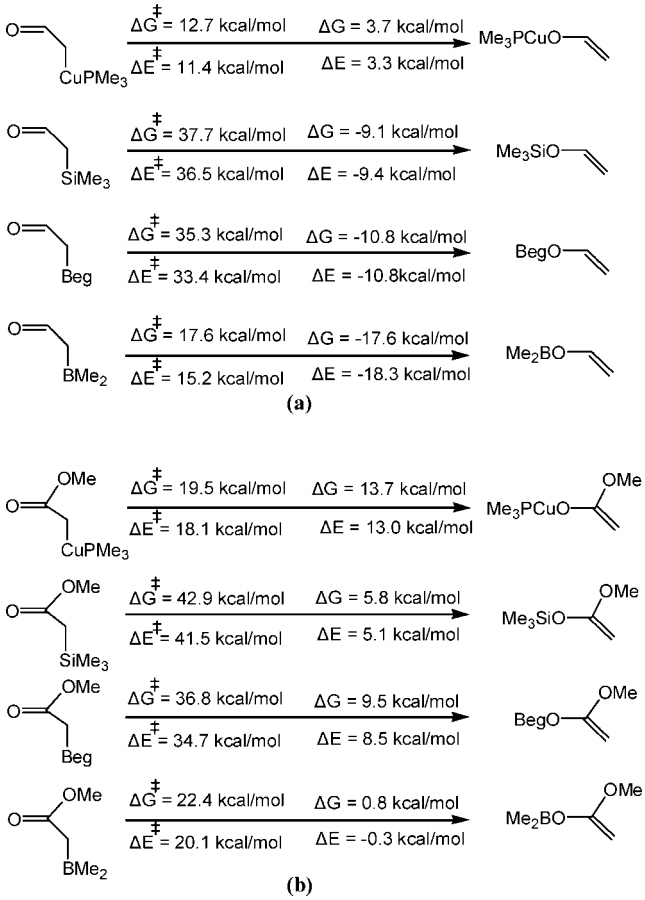

the enol intermediate **4A** (also called an O-enolate) is only slightly less stable, by 2.7 kcal/mol, than the keto intermediate **3A** (also called a C-enolate). The barrier (11.0 kcal/mol) for their interconversion is also relatively small. For methylacrylate, the O-enolate **4Aester** is much less stable, by 14.7 kcal/mol, than the C-enolate **3Aester**. The barrier (16.7 kcal/mol) for their interconversion is also much greater.

In order to gain insight into the relative stability of the C- and O-enolates discussed above, we investigated the thermodynamic and kinetic stability of C- and O-enolates, $O{=}CHCH_2E$ (or $O{=}C(OMe)CH_2E$) and $EO{-}CH{=}CH_2$ (or $EO{-}C(OMe){=}CH_2$), respectively, having E = $CuPMe_3$, $SiMe_3$, Beg and BMe_2. Earlier theoretical studies showed that when E = H, the "O-enolate" (i.e., the enol), $HOCH{=}CH_2$ is higher in energy than the "C-enolate" (i.e., the aldehyde), $O{=}CHCH_3$ by 9.4 kcal/mol.[21] When E = $CuPMe_3$, the O-enolate $(PMe_3)CuOCH{=}CH_2$ is less stable than the C-enolate $O{=}CHCH_2CuPMe_3$ by only 3.7 kcal/mol (Scheme 6a). When E = $SiMe_3$, Beg, and BMe_2, the O-enolates become more stable than the corresponding C-enolates (Scheme 6a). The results show that strong E−O bonds stabilize the O-enolates. The interconversion barriers seem to be related to two factors. When E = $CuPMe_3$, the interconversion barrier was calculated to be the smallest. Cu is the largest in size, giving rise to the least significant ring strain in the four-membered-ring transition state.

(3) (a) Alkene diboration: Baker, R. T.; Nguyen, P.; Marder, T. B.; Westcott, S. A *Angew. Chem., Int. Ed. Engl.* **1995**, *34*, 1336. (b) Ishiyama, T.; Yamamoto, M.; Miyaura, N. *Chem. Commun.* **1996**, 2073. (c) Iverson, C. N.; Smith, M. R., III *Organometallics* **1997**, *16*, 2757. (d) Ishiyama, T.; Yamamoto, M.; Miyaura, N. *Chem. Commun.* **1997**, 689. (e) Dai, C.; Robins, E. G.; Scott, A. J.; Clegg, W.; Yufit, D. S.; Howard, J. A. K.; Marder, T. B. *Chem. Commun.* **1998**, 1983. (f) Marder, T. B.; Norman, N. C.; Rice, C. R. *Tetrahedron Lett.* **1998**, *39*, 155. (g) Ishiyama, T.; Momota, S.; Miyaura, N. *Synlett* **1999**, 1790. (h) Mann, G.; John, K. D.; Baker, R. T. *Org. Lett.* **2000**, *2*, 2105. (i) Nguyen, P.; Coapes, R. B.; Woodward, A. D.; Taylor, N. J.; Burke, J. M.; Howard, J. A. K.; Marder, T. B. *J. Organomet. Chem.* **2002**, *652*, 77. (j) Morgan, J. B.; Miller, S. P.; Morken, J. P. *J. Am. Chem. Soc.* **2003**, *125*, 8702. (k) Ramírez, J.; Corberán, R.; Sanau, M.; Peris, E.; Fernández, E. *Chem. Commun.* **2005**, 3056. (l) Trudeau, S.; Morgan, J. B.; Shrestha, M.; Morken, J. P. *J. Org. Chem.* **2005**, *70*, 9538. (m) Corberán, R.; Ramírez, J.; Poyatos, M.; Perisa, E.; Fernández, E. *Tetrahedron: Asymmetry* **2006**, *17*, 1759. (n) Lillo, V.; Fructos, M. R.; Ramírez, J; Díaz Requejo, M. M.; Pérez, P. J.; Fernández, E. *Chem.-Eur. J.* **2007**, *13*, 2614.

(4) (a) Alkyne diboration: Ishiyama, T.; Matsuda, N.; Miyaura, N.; Suzuki, A *J. Am. Chem. Soc.* **1993**, *115*, 11018. (b) Ishiyama, T.; Matsuda, N.; Murata, M.; Ozawa, F.; Suzuki, A.; Miyaura, N. *Organometallics* **1996**, *15*, 713. (c) Lesley, G.; Nguyen, P.; Taylor, N. J.; Marder, T. B.; Scott, A. J.; Clegg, W.; Norman, N. C. *Organometallics* **1996**, *15*, 5137. (d) Iverson, C. N.; Smith, M. R. *Organometallics* **1996**, *15*, 5155. (e) Thomas, R. L.; Souza, F. E. S.; Marder, T. B. *J. Chem. Soc., Dalton Trans.* **2001**, 1650. (f) Ali, H. A.; Quntar, A. E. A. A.; Goldberg, I.; Srebnik, M. *Organometallics* **2002**, *21*, 4533. (g) Braunschweig, H.; Kupfer, T.; Lutz, M.; Radacki, K.; Seeler, F.; Sigritz, R. *Angew. Chem., Int. Ed.* **2006**, *45*, 8048.

(5) (a) C=O diboration: Laitar, D. S.; Muller, P.; Sadighi, J. P. *J. Am. Chem. Soc.* **2005**, *127*, 17196. (b) Laitar, D. S.; Tsui, E. Y.; Sadighi, J. P. *J. Am. Chem. Soc.* **2006**, *128*, 11036. (c) For an example of N=N diboration, see: Braunschweig, H.; Kupfer, T. *J. Am. Chem. Soc.* **2008**, *130*, 4242.

(6) (a) Cui, Q.; Musaev, D. G.; Morokuma, K *Organometallics* **1997**, *16*, 1355. (b) Cui, Q.; Musaev, D. G.; Morokuma, K. *Organometallics* **1998**, *1* (7), 742. (c) Cui, Q.; Musaev, D. G.; Morokuma, K. *Organometallics* **1998**, *17*, 1383. (d) For a review, see: Huang, X.; Lin, Z. In *Computational Modeling of Homogeneous Catalysis*; Maseras, F., Lledós, A., Eds.; Kluwer Academic Publishers: Amsterdam, 2002; pp 189−212.

(7) (a) General mechanism: Zhao, H. T.; Lin, Z. Y.; Marder, T. B *J. Am. Chem. Soc.* **2006**, *128*, 15637. (b) Dang, L.; Zhao, H. T.; Lin, Z. Y.; Marder, T. B *Organometallics* **2007**, *26*, 2824. (c) Dang, L.; Zhao, H. T.; Lin, Z. Y.; Marder, T. B *Organometallics* **2008**, *27*, 1178. (d) Zhao, H. T.; Dang, L.; Lin, Z. Y.; Marder, T. B. *J. Am. Chem. Soc.* **2008**, *130*, 5586.

(8) (a) α,β-Unsaturated carbonyl diboration: Ito, H.; Yamanaka, H.; Tateiwa, J.; Hosomi, A *Tetrahedron Lett.* **2000**, *41*, 6821. (b) Ali, H. A.; Goldberg, I.; Srebnik, M. *Organometallics* **2001**, *20*, 3962. (c) Takahashi, K.; Ishiyama, T.; Miyaura, N. *Chem. Lett.* **2000**, *982*. (d) Takahashi, K.; Ishiyama, T.; Miyaura, N. *J. Organomet. Chem.* **2001**, *625*, 47. (e) Kabalka, G. W.; Das, B. C.; Das, S. *Tetrahedron Lett.* **2002**, *43*, 2323. (f) Mun, S.; Lee, J.; Yun, J. *Org. Lett.* **2006**, *8*, 4887. (g) Hirano, K.; Yorimitsu, H.; Oshima, K. *Org. Lett.* **2007**, *9*, 5031. (h) Lee, J.-E.; Kwon, J.; Yun, J. *Chem. Commun.* **2008**, 733. (i) Lee, J.-E.; Yun, J. *Angew. Chem., Int. Ed.* **2008**, *47*, 145.

(9) (a) Lawson, Y. G.; Lesley, M. J. G.; Marder, T. B.; Norman, N. C.; Rice, C. R. *Chem. Commun.* **1997**, 2051. (b) Bell, N. J.; Cox, A. J.; Cameron, N. R.; Evans, J. S. O.; Marder, T. B.; Duin, M. A.; Elsevier, C. J.; Baucherel, X.; Tulloch, A. A. D.; Tooze, R. P. *Chem. Commun.* **2004**, 1854.

(10) (a) Becke, A. D. *J. Chem. Phys.* **1993**, *98*, 5648. (b) Miehlich, B.; Savin, A.; Stoll, H.; Preuss, H. *Chem. Phys. Lett.* **1989**, *157*, 200. (c) Lee, C.; Yang, W.; Parr, G. *Phys. Rev. B* **1988**, *37*, 785. (d) Stephens, P. J.; Devlin, F. J.; Chabalowski, C. F. *J. Phys. Chem.* **1994**, *98*, 11623.

(11) (a) Fukui, K. *J. Phys. Chem.* **1970**, *74*, 4161. (b) Fukui, K. *Acc. Chem. Res.* **1981**, *14*, 363.

(12) Krishnan, R.; Binkley, J. S.; Seeger, R.; Pople, J. A. *J. Chem. Phys.* **1980**, *72*, 650.

(13) (a) Wachters, A. J. H. *J. Chem. Phys.* **1970**, *52*, 1033. (b) Hay, P. J. *J. Chem. Phys.* **1977**, *66*, 4377.

(14) (a) Gordon, M. S. *Chem. Phys. Lett.* **1980**, *76*, 163. (b) Hariharan, P. C.; Pople, J. A *Theor. Chim. Acta* **1973**, *28*, 213. (c) Binning, R. C., Jr.; Curtiss, L. A. *J. Comput. Chem.* **1990**, *11*, 1206.

(15) Frisch, M. J.; et al. *Gaussian 03, revision B.05*; Gaussian, Inc.: Pittsburgh, PA, 2003.

(16) (a) Lin, Z. *Coord. Chem. Rev.* **2007**, *251*, 2280, and references therein. (b) Ng, S. M.; Lam, W. H.; Mak, C. C.; Tsang, C. W.; Jia, G.; Lin, Z.; Lau, C. P. *Organometallics* **2003**, *22*, 641. (c) Lam, W. H.; Jia, G.; Lin, Z.; Lau, C. P.; Eisenstein, O *Chem. Eur. J.* **2003**, *9*, 2775.

(17) Vastine, B. A.; Hall, M. B. *J. Am. Chem. Soc.* **2007**, *129*, 12068.

(18) Bader, R. F. W. *Atoms in Molecules: A Quantum Theory*; Oxford University Press: New York, 1990.

(19) (a) Oxgaard, J.; Muller, R. P.; Goddard, W. A., III; Perianna, R. A. *J. Am. Chem. Soc.* **2004**, *126*, 352. (b) Oxgaard, J.; Perianna, R. A.; Goddard, W. A., III *J. Am. Chem. Soc.* **2004**, *126*, 11658.

(20) Perutz, R. N.; Sabo-Etienne, S. *Angew. Chem., Int. Ed.* **2007**, *46*, 2578.

(21) (a) Rodríguez-Santiago, L.; Vendrell, O.; Tejero, I.; Sodupe, M.; Bertran, J. *Chem. Phys. Lett.* **2001**, *334*, 112. (b) Solans-Monfort, M.; Bertran, J.; Branchadell, V.; Sodupe, M. *J. Phys. Chem. B* **2002**, *106*, 10220.

A two-coordinate Cu(I) center has low-lying available empty p orbitals, allowing the metal center to maintain interactions with both C and O in the transition state. When E = BMe_2, the interconversion barrier was calculated to be the second smallest. Apparently, the empty p orbital on the boron center plays the most important role in stabilizing the transition state. A significant interconversion barrier was calculated for the case when E = Beg, suggesting that the "empty" orbital on the boron center in this case is "saturated" by interacting with the occupied oxygen p orbitals of the eg group. When E = $SiMe_3$, the largest barrier was calculated because the silicon center lacks readily available, low-lying, empty orbitals.

Scheme 6b gives the results calculated for the analogous systems containing an ester group. The trend in the interconversion barriers and in the reaction energies follows that discussed above. Significantly higher interconversion barriers are calculated. The interconversions are all endothermic except in the case of E = BMe_2, in which the interconversion is approximately thermodynamically neutral. These results are due to the relatively inert ester group.

Conclusions

The detailed mechanism for the borylation of α,β-unsaturated carbonyl compounds acrolein and methylacrylate, catalyzed by (PMe_3)Cu(Beg), has been investigated with the aid of DFT calculations.

For the borylation of acrolein, the computational results show that the catalyzed reaction occurs through C═C insertion into Cu−B to give a β-borylalkyl C-bound Cu(I) enolate intermediate followed by a keto-to-enol isomerization to the O-bound Cu(I) enolate, and a subsequent σ-bond metathesis with a diboron reagent.

In the acrolein insertion, the Cu−B bond of the phosphine copper(I) boryl complex is preferentially added across the C═C double bond of the acrolein to form a β-borylalkyl C-bound Cu(I) enolate intermediate. The regioselectivity in the insertion is attributed to the fact that the β-carbon, i.e., the terminal carbon, of acrolein is the most electrophilic site and the boryl ligand in the phosphine copper(I) boryl complex acts as a nucleophile during the insertion process. The calculations show that a direct metathesis between the β-borylalkyl Cu(I) intermediate, which contains a Cu−C bond, and a diboron reagent does not occur to give a 3,4-addition diboration product. Instead, the intermediate undergoes a keto-to-enol isomerization to give an O-bound Cu-enolate intermediate with comparable stability, from which a metathesis reaction with the diboron reagent then occurs to give the 1,4-addition diboration product. These results are related to the fact that metathesis between Cu−O and B−B is much easier than that between Cu−C and B−B.[7d] We also studied the role of methanol or water on the catalytic reactions and found that the presence of methanol will not affect the reactivity of the copper(I) boryl active species and alcoholysis or hydrolysis can also occur with both the C- and O-bound Cu(I) enolate intermediates.

Comparison of the insertion reactions of ethene, formaldehyde, and acrolein shows that the insertion barriers correlate very well with the orbital energies of the LUMOs calculated for the three substrates, confirming the notion that the insertion mainly involves a nucleophilic attack of the Cu−B σ bond on the coordinated unsaturated substrate molecule. Although formaldehyde is more reactive than ethene in the insertion reaction, the reactivity of the C═C bond is greater than that of the C═O bond in α,β-unsaturated aldehydes.

For the borylation of methylacrylate, our calculations allow us to gain insight into why methanol additives are essential for successful β-borylation of α,β-unsaturated esters as found experimentally.[8f] Due to the inertness of the ester group, a keto-to-enol isomerization does not occur in the C-bound Cu(I) enolate intermediate derived from the C═C insertion into Cu−B. Instead, alcoholysis (or hydrolysis) occurs directly on the C-bound Cu(I) enolate intermediate to give the borylation product and (PMe_3)Cu-OMe. From (PMe_3)Cu-OMe, σ-bond metathesis with a diboron reagent regenerates the copper(I) boryl active species.

The different borylation reaction mechanisms of acrolein and methylacrylate are closely related to the relative thermodynamic and kinetic stability of the C- and O-enolate intermediates involved in the reactions of the two different classes of substrates. Likewise, for O═$CHCH_2$E vs EO−CH═CH_2, strong E−O bonds stabilize the O-bound enolates for E = B and Si, whereas the C-bound enolate is more stable for E = Cu(PMe_3). Interconversion barriers are governed by the presence or absence of a suitable empty orbital on E and the size of the Cu atom. For O═C(OMe)CH_2E vs EO−C(OMe)═CH_2, the C-bound enolates are more stable except for E = BMe_2, and the interconversion barriers are all significantly higher than those for the O═$CHCH_2$E vs EO−CH═CH_2 case.

Acknowledgment. This work was supported by the Research Grants Council of Hong Kong (HKUST 601507). T.B.M. thanks the Royal Society (UK) for support via an International Outgoing Short Visit Grant.

Supporting Information Available: Complete ref 15 and tables giving Cartesian coordinates and electronic energies for all of the calculated structures. This material is available free of charge via the Internet at http://pubs.acs.org.

OM8006294